Powder Technology 448 (2024) 120294

Contents lists available at ScienceDirect

Powder Technology

journal homepage: www.journals.elsevier.com/powder-technology

Examining particle size growth in twin screw granulation up to steady state with acoustic emissions

H.A. Abdulhussain, M.R. Thompson *

CAPPA-D/MMRI, Department of Chemical Engineering, McMaster University, Hamilton, Ontario, Canada

HIGHLIGHTS

- Granulation at a higher degree of fill (DF) becoming increasingly dependent on the kneading zone.
- Steady state will be reached by 5 times the mean residence time independent of DF.
- Inline PAT can output a representative particle size distribution with only 5 s sampling.

GRAPHICAL ABSTRACT

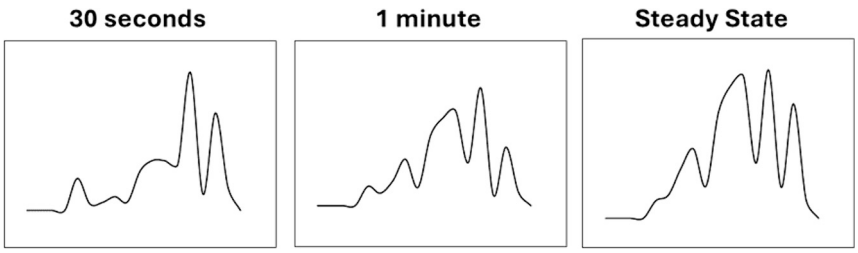

ARTICLE INFO

Keywords:
Acoustic emissions
Process analytical technology
Transient flow state
Twin screw granulation
Granulation mechanism

ABSTRACT

The transient evolution of granules was studied to learn new details about the underlying mechanism for continuous wet granulation in a twin-screw extruder. Sieving and a new inline PAT for particle size development was used to gain these insights. The onset for steady state was established based on observing a consistent PSD, which occurred at five times the mean residence time of the process, over a range of degrees of fill (DF; 12–30 %). The early stages of startup for granulation were captured by the inline PAT, showing different stages of granule growth for particle sizes ranging from 102 to 2230 μm. The analysis found that conveying elements have a stronger influence on granule growth at a low DF whereas the kneading zone had a stronger influence on granule growth at a higher DF. This study presents new details on this black-box process while highlighting the unique value of PAT to twin-screw granulation.

1. Introduction

In the pharmaceutical industry, most global regulatory bodies are encouraging the development of advanced quality control strategies around the manufacturing of drug products, with specific focus on continuous processes. Twin screw granulation has gained significant interest from the pharmaceutical industry as one such process over this past decade [1]. Twin screw granulation (TSG) offers significant advantages over comparable high shear batch processing, including systematic integration with other unit operations, increased throughput, shorter process (residence) time, and higher product consistency [2,3].

The transition to steady state in TSG has gone unstudied to date because the process operates as a black-box and most of our available characterization tools need substantial sample sizes to draw conclusions and yet this period of time may reveal significant details about the granulation mechanism. Understanding how granule sizes evolve during this early period up till a steady particle size distribution is obtained, should better highlight the mechanism inside this machine, which is

* Corresponding author.
E-mail address: mthomps@mcmaster.ca (M.R. Thompson).

https://doi.org/10.1016/j.powtec.2024.120294
Received 5 July 2024; Received in revised form 10 September 2024; Accepted 15 September 2024
Available online 18 September 2024

often described using the classical stages of nucleation, propagation and granule breakage seen in batch processes [4,5] without evidence that they accurately describe what is taking place inside the extruder (especially its compression zone). The transient period may be too short to fully address our gaps in knowledge about this process, but its study has the potential to add new information on a continuous processing method that has just begun to produce commercial drugs. The complexity of the process is attributed to the confounding influences of its process variables, including formulation properties [6,7], screw design [7,8], screw speed [9], mass flowrate [4,10], and liquid-to-solids (L/S) ratio [9,11]. These variables are strongly affected by the degree of fill (DF), with the granulation mechanism seemingly changed as a result. By the process mapping done to date it has been observed that at lower DF, granules are thought to experience less frictional forces and are able to move freely in the barrel, which allows for increased growth and consolidation [6,12]. Conversely, at higher DF, granules are more constrained, moving in a plug-like manner, which is believed to reduce the number of particles being wetted and yielding more fines produced [13–15]. Shi [16] confirmed this transition in the granulation mechanism was around a DF of 20 %, observed in both 18 mm and 27 mm twin-screw granulators, where the impact of screw speed on the PSD below this DF is more prominent than the mass flow rate, and vice versa above this value. Seem et al. [14] also mentioned in their review that screw speed does have an impact on granulation at very high DF (we estimate at 60 % DF and onwards), which indicates that effects of screw speed may only be prominent at the extremes (very low or high DF) from a process mapping standpoint.

The only studies known to have been explicitly concerned with whether the process in a TSG was steady, relied on torque measurements and then only in a GEA ConSigma® machine [9,11,14,17]. While torque is a helpful variable to monitor operational consistency and will have some indirect correspondence to the state of the compression zone where binder spreading and particle agglomeration will primarily be occurring, it is not a direct descriptor of output performance such as end product responses like fracture strength and dissolution rate, or the more universally required information like particle size distribution (PSD). In fact, Ryckaret et al. [18], who provided some of the most thorough studies on the effects of torque in twin-screw granulation, concluded that its inline measurement cannot be used to monitor particle size. Additionally, none of these studies examined what was happening inside the TSG during the transition period in their machines.

The purpose of this study was to explore the evolution of granulation during the transient start-up period after first establishing when steady state occurred for the PSD. The work compares the capabilities of off-line sieve classification versus a recently developed inline PAT based on acoustic emission (AE) [19] to understand how PSD evolves in a twin-screw granulator. The term PAT in this paper refers to an inline acoustic sensor coupled with a trained artificial intelligence (AI) model. The goals of the research were to assess the value of inline systems on their capacity to observe phenomena in a continuous process on a very short timescale. This study was also the first opportunity to relate mean residence time (MRT) to the time to reach steady state in a twin-screw granulator, which is commonly understood information for other chemical processes [20–23].

2. Materials and methods

2.1. Materials

All trials were conducted with a placebo formulation of 60 wt% Flowlac® 100 lactose monohydrate (Meggle Pharma; Germany), 20 wt% Avicel® PH-102 microcrystalline cellulose (International Flavors and Fragrances; USA), and 20 wt% Kollidon SR® polyvinyl acetate/povidone (BASF; USA). The formulation was pre-mixed and then dried at 50 $^{\circ}C$ for 24 h before use. The binder solution consisted of 2 wt% METHOCEL E3PLV (International Flavors and Fragrances; USA) dissolved in distilled water.

2.2. Twin screw granulation experiments

Wet granulation was conducted in a 27 mm 40 L/D co-rotating twin-screw extruder, model ZSE-27HP from Leistritz Extrusion (Somerville, NJ). The extruder consisted of 10 barrel zones, with the first zone (Z0) being water cooled followed by nine (Z1-Z9) temperature controlled zones. A standard granulation screw design was employed with conveying elements going from Z0 – Z7, two kneading blocks (60^{o} offset, medium thickness elements) in Z8 and then followed by another set of conveying elements in Z9, as seen in Fig. 1. This screw design was used for all experiments. The barrel temperature was set to 15 $^{\circ}C$ to avoid the low glass transition temperature (35 $^{\circ}C$ according to the manufacturer [24]) of Kollidon SR®. The formulation was fed into the extruder using a Brabender T20 twin screw gravimetric feeder (Missisauga, ON, Canada) and the liquid binder was added by an ISCO 260D high syringe pump (Teledyne-ISCO Inc.; Lincoln, NE) at zone Z3.

The degree of fill was controlled at 12 % (Low DF) or 30 % (High DF) to operate the TSG on either side of one of the known granulation mechanism transition first noted by Seem et al. [14] and Tu et al. [15] and then further quantified by Shi [16] (~20 % DF). The degree of fill was calculated according to the best-fit regressed model developed by Mozumder [25] for our 27 mm 40 L/D extruder, who used a fixed L/S ratio of 26 % while varying screw speed (SS) and powder (mass) flowrate (PFR):

$$DF = -0.07(SS) + 9.2\,(PFR) + 8.8 \quad (1)$$

For the current trials, the lower and upper bounds of the PFR were set as 3 kg/h and 4.5 kg/h (due to material constraints), respectively and then adjusting screw speed using Eq. (1) so that the system operated at the appropriate DF, above or below the transition value of ~20 %. The chosen DF for this work were 12 % (349 RPM and 3 kg/h) and 30 % (288 RPM and 4.5 kg/h).

For the trials determining when steady state occurred, the L/S ratio was kept at 27 %. The DF should not be significantly changed by the L/S being different from the operating state used to generate Eq. (1), since it has been shown that DF is mainly a function of screw speed, mass flowrate, and screw design [14,26]. “Startup” procedure meant turning on the motor to the desired screw RPM, while simultaneously turning on the liquid pump and the feeder. Granules were collected from startup to 30 s (0–30 s), then the feeder, pump, and screw were then stopped. The machine was cleaned out of particle and then started again. This approach was used for startup to 1 min (0–60 s or 0–1 min) and startup to 2 min (0–120 s or 0–2 min). For every other startup period afterwards (namely 2–4 min, 4–6 min, 6–8 min, 8–10 min), granules were only collected over the last 2 min of the mentioned period. The reason for 2 min of sampling was that it was the minimum amount of time needed to collect approximately 100 g of granules for further sieve characterization at both DF conditions. Once the onset of steady state was determined for PSD, additional trials at 18 % and 39 % L/S ratio were conducted for artificial intelligence (AI) model training of the PAT (referring to Sec. 2.5 below) with granules collected at 2 and 4 min, respectively. The two L/S used for AI model training were selected to generate particle size distributions with larger amounts of fine (<300 μm) or coarse granules (>2100 μm).

All granule samples collected from the trials mentioned, were placed in trays and were left to air dry at room temperature for 48 h for offline analysis of their PSDs. Approximately 1–2 g of granules collected before air drying were analyzed for their moisture content, collected from the trials of runtime at 0–30 s, 0–1 min, 0–2 min, and 2–4 min, for all L/S ratios at both low and high DF. The moisture content was measured using a HG63 moisture analyzer (Mettler-Toledo; Columbus, OH).

Steady state residence time distributions were evaluated at 10 min

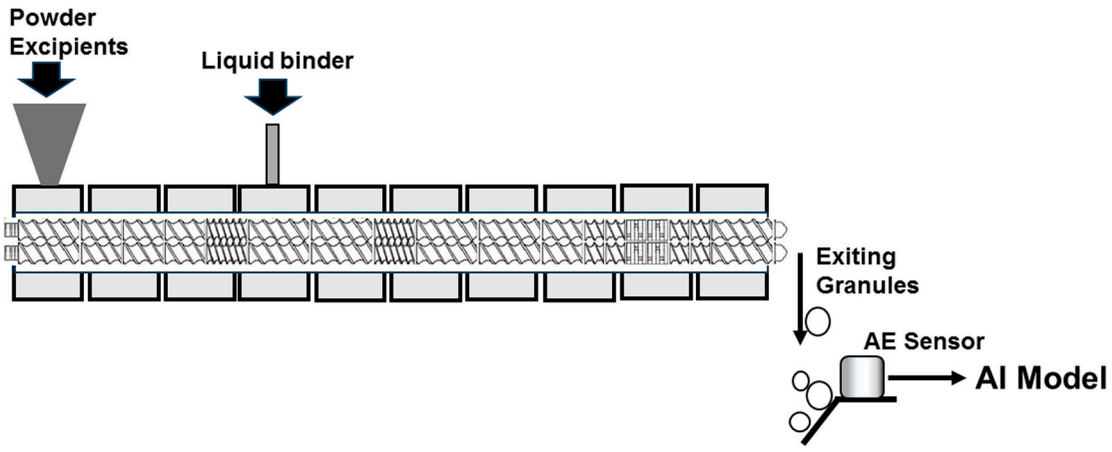

Fig. 1. Screw design used for twin-screw granulation experiments.

after startup for the 27 % L/S ratio condition, by introducing a color tracer of 1 g cocoa powder into the extruder as a pseudo dirac pulse to calculate the MRT at 12 % and 30 % DF. Triplicates of the MRT were performed to determine uncertainty.

2.3. Offline particle size distribution characterization

The offline analysis of PSD was performed using a Ro-Tap RX-29 sieve shaker (W.S. Tyler; Mentor, OH). Extruded samples sat in aluminum trays from when they were dried, requiring sampling using a scoop to collect particles from near both the top and bottom of the tray, compensating for settling during storage. Unless otherwise stated, 100 g of granules from a trial were first classified into eight fractions using a set of sieves with nominal openings of 2100, 1700, 1400, 1180, 500, 300 μm along with the pan at the bottom. The sieve stack was mechanically agitated for 5 min before weighing the sieves to determine the PSD. The mass on the 2100 μm sieve was further classified with a second set of sieves with nominal openings of 8000, 6300, 4760, 3350, 2360, 2100, and 1700 μm and agitated for 5 min before weighing. Similarly, the mass in the bottom pan from the first classification was further classified with a third set of sieves with nominal openings of 500, 300, 250, 180, 150, 53, and 44 μm and agitated for 5 min before weighing. This procedure was done to obtain a well defined PSD. As a result, the weight fractions shown in this work are for the average sizes of 7150, 5530, 4055, 2855, 2230, 1900, 1550, 1290, 1015, 675, 400, 275, 215, 165, 102, and 49 μm.

For sample collection from 0 to 30 s or 0–1 min, the amount of mass being sieved was well below 100 g, and so a sensitivity test was conducted in this study to determine the minimum amount of mass needed to reproducibly measure the PSD using the sieving technique. Samples at 27 % L/S collected at different time intervals were mixed together, making a total mass of 600 g. The sample was agitated manually for 2 min before 100 g of material were extracted and characterized using the first set of sieves mentioned above. This procedure was repeated but now extracting either 50g, 20 g, or 10 g of material and sieving to determine PSD.

2.4. Fracture strength

Fracture strength of the granules was determined by uniaxial compression with an Instron 3366 benchtop mechanical testing system (Instron Corporation; Canton, MA) following the method by Adams [27]. A small quantity of granules (0.6 g) in the particle size range of 400–1900 μm was placed in a die press with a 11.09 mm bore diameter and were compressed at a 3.5 mm/min until a maximum load of 4200 N was reached. The stress-strain curve was then analyzed to obtain the fracture strength according to Eq. (2) at high values of compressive strain (above ~20 %):

$$lnP = ln\left(\frac{\tau'}{\alpha'}\right) + \alpha'\varepsilon + ln(1 - exp(-\alpha'\varepsilon)) \quad (2)$$

where P is the compressive stress, α' is the lateral stress pressure coefficient, τ' is the characteristic fracture strength, and ε is the compressive strain. The measurement was repeated three times to determine the uncertainty.

3. Inline acoustic emission PAT validation

Inline determination of the particle size distributions exiting the TSG is described in our earlier studies using an acoustic emissions (AE) technique [19,28]. The acoustic sensor combined with AI model making up the PAT, can estimate the full bimodal size distribution indicative of TSG processing, giving much more information than just simple single value descriptors like d_{50}. Briefly, a stainless steel impact plate was positioned 20 cm below the outlet of the extruder with an F15α broadband AE sensor (Physical Acoustics, Princeton, NJ) attached using high vacuum grease (Dow Corning) onto a tab protruding from the plate. The sensor detected only ultrasonic frequencies, with greatest sensitivity between 100 and 450kHz (where most particle emissions occurred for this process) and no sensitivity to the audible noises related to lab machinery [29]. The detected acoustic signal was amplified using a Physical Acoustics 2/4/6c amplifier set to +60 dB and collected at an acquisition rate of 3 MHz for all experiments. For the steady state determination trials at 27 % L/S, the AE signal was continuously collected at 10 min after startup whereas for the trials at 18 and 39 % L/S, the signal was collected at 6 min from startup. An auditory masking filter coupled to a Walton-Braun impact model was used to correct for sound attenuation based on particle size and moisture content, as described in a previous study [19]. A Haar wavelet filter was used to remove any excess noise from the signal and a fast Fourier transform was used to convert the signal from the time domain into the frequency domain. A neural network AI model translates the filtered amplitude-frequency signal in the 0–700 kHz range into a particle size distribution. To improve the accuracy of the model built on previous data [19,28] for the current formulation, 30 s sampled segments of the AE signal corresponding to times of granule collection for the current formulation along with their corresponding sieved particle size data were used for model retraining. The collected granules corresponded to steady state were obtained between 2 and 4 min during a trial run for 18 %, 27 %, and 39 % L/S at both DFs for this placebo formulation. The AI model was trained for 300 iterations or epochs, with 80 % of the data used for training and 20 % for testing. The model was trained three times with different training and testing datasets to estimate the uncertainty of the model output. After training, the model was able to monitor the PSD

accurately with the largest error corresponding to the 215μm weight fraction (at a low degree of fill) with a root mean squared error (RMSE) of 0.61 wt% using data from the testing set. This meant the model could accurately predict a PSD over the L/S ratios and degrees of fill used in the study (and hence the changes in composition and density of particles impacting the plate housing the acoustic sensor). The uncertainty in this testing was presented as a standard deviation in reported PSD for this study.

In the earlier studies developing the method [19,28], the AI model was established by analyzing 30-s segments of the signal, which was chosen as a period of time to maximize the number of particle collisions used to estimate the PSD while providing timely updates to operators; the 30 s corresponded closely to the MRT in most cases. In the present study, the intent of using this method was to understand the nature of granules exiting the TSG well under the first minute of running the machine and that meant analyzing much smaller segments of the collected signal than even 30 s. Since the signal is a recording of every particle impact over time and therefore, records an accurate PSD corresponding to whatever time segment is analyzed, the concern here was how the AI model handled the smaller datasets. To explore the segment size of the signal required to match an offline characterization of PSD, a sensitivity analysis was performed. The estimated PSD by the AI model were compared using shorter signal segments from within the normal 30 s recording, taken from the AE signal between 3.5 and 4 min after startup, namely segment intervals of 0–1 s, 0–5 s, 0–10 s, 0–20 s, and 0–30 s. The corresponding outputs of the model are shown in Fig. 2 along with the offline sieved distribution for a sample taken between 2 and 4 min of run time at 27 % L/S ratio and 12 % DF.

The estimated distributions determined by the AI model showed the only major deviation from the sieved data was when working with a time segment of 1 s duration (0–1 s interval), with the largest RMSE being for the ungranulated fractions, 215μm and 102 μm at 3.1 wt% and 2.0 wt%, respectively. For a time segment of 5 s (0–5 s interval), the maximum RMSE decreased to 1.2 wt% and remained consistently below 1.0 wt% with the analysis of larger time segments from the AE signal; a RMSE value below 1 wt% is considered ideal for the model. In general, the larger the size of the signal segment analyzed by the AI model, the more accurate is the estimation. However, a segment of 10 s (or longer) was considered sufficiently close to match a sieved distribution collected over the span of 2 min, with a maximum RMSE below 1.0 wt% across all particle sizes. Therefore, a signal segment of 10 s, recording the exit of 8.3 g granules and corresponding to 58 screw revolutions, appears sufficient to record enough particle collision to get the correct normalized distribution shape (at steady state).

Based on this analysis, there was confidence in using the inline acoustic sensor to analyze the transient period during startup, so long as the analysis was not less than 5 s and with good confidence when considering a period of at least 10 s.

4. Results and discussion

No method of determining the particle size distribution of a sample is without limitations from measuring its true nature. The method of sieving requires a detectable quantity of mass on each tray, per the sensitivity of the weigh scale and weight of the sieves themselves, and even then, each tray is capturing particles covering a range of sizes assumed to be spherical in shape [30,31]. The new acoustic emissions PAT records the emitted elastic waves generated by wet granules exiting the extruder and impacting a plate, and its AI model to translate the signal into a PSD is trained with the classified samples obtained by sieving once dry. And so, neither approach was considered to more accurately representing the particle size distribution from the twin-screw granulator. The important difference in this study was that the inline acoustic sensor, as an accurate recording of every particle impact, could display distributions of very few particles and therefore analyze the time period during startup of the TSG before steady state was reached.

4.1. Sieving technique sensitivity

To use sieved data in this study, the reliability of the method to characterize PSD with samples below the traditional amounts of 80–100 g used [32–34] was assessed on account of the short run times being considered. Fig. 3 shows multiple PSDs when the sample size was reduced from 100 g all the way down to 10 g, whereas Table 1 shows the d_{10}, d_{50}, and d_{90} for each of those distributions. Interestingly, the shape of the distribution showed little changes as the sample size decreased from 100 g to 50 g to 20 g, and only showed a significant difference at 10 g. A gradual decrease is seen in d_{10}, d_{50}, and d_{90} values from 100 g to 20 g, with the largest decrease of roughly 8.5 % in d_{50} over that range. Below 20 g, there was a shift in trend with the d_{50}, and d_{90} increasing whereas the d_{10} continued to decrease.

Based on these test results, from a reliability perspective, the minimum amount of mass that was considered for particle characterization

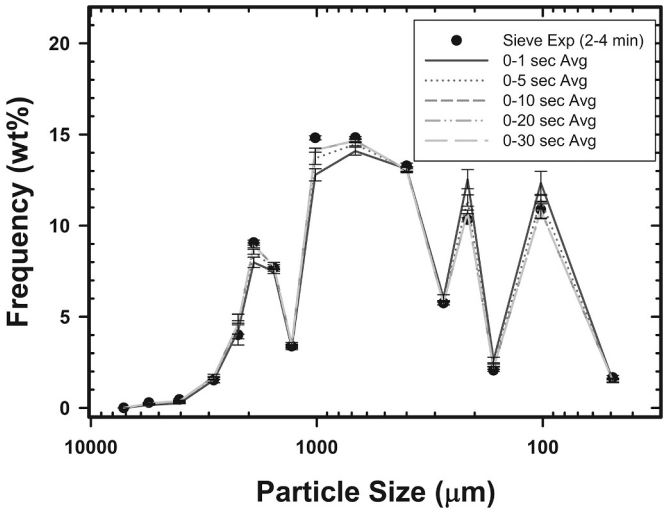

Fig. 2. Estimated PSD generated by the AI model using varied time segments of an AE signal collected from 3.5 to 4 min after startup for the trial conditions of 12 % DF and 27 % L/S ratio. Error bars for the offline sieved data and PAT estimates represent the standard deviation (n = 3).

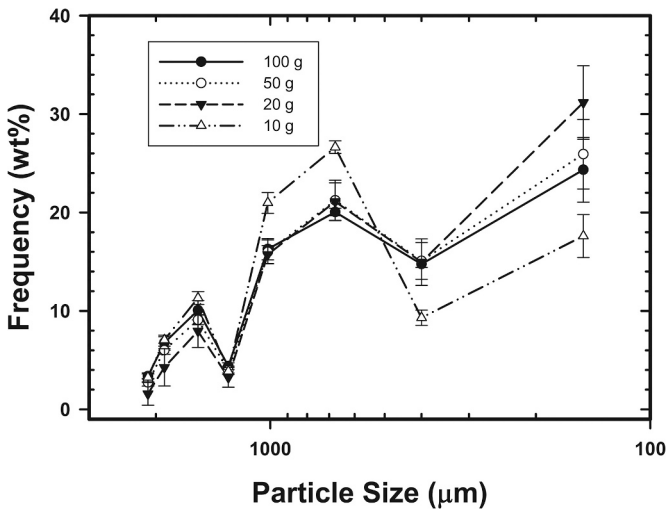

Fig. 3. Particle size distribution sieved with 100, 50, 20, and 10 g of granulated material. Displayed distributions are incrementally shifted on the y-axis to clearly show the evolution of the distribution shape with sampled amount. Error bars represent the standard deviation (n = 3).

Table 1
Single descriptors and their standard deviations for the particle size distributions sieved with varying masses.

Mass Sieved (g)	d_{10} (μm)	d_{50} (μm)	d_{90} (μm)
100	1901 ± 30	859 ± 57	342 ± 5
50	1851 ± 32	816 ± 59	339 ± 5
20	1771 ± 68	786 ± 47	332 ± 4
10	1706 ± 361	860 ± 207	348 ± 21

in this study was 20 g. which is close to the amount that exits from the extruder over 30 s at the chosen lower DF of this study.

4.2. Steady state determination

To examine the transient state, one must first determine when steady state occurs, at least covering the lower bounds of DF for wet granulation in the TSG. It was advantageous to describe the onset of steady operations relative to the residence time of the machine, following standard practices of Chemical Engineering [20–23]. Using offline and inline particle size characterizations of granules collected, Fig. 4 compares the size distributions of samples from startup until 10 min at 27 % L/S ratio while Fig. 5 presents the d_{10}, d_{50}, and d_{90} of those distributions as a function of time, through sieving and AE PAT. Based on the limits of sieve classification disclosed in Section 4.1 and the flowrates chosen (3 and 4.5 kg/h), it took ~24 and 16 s respectively to reach 20 g of granules so nothing was evaluated below 30 s for these specific trials but since reaching steady state took longer, it did not impact the analysis. Since the typical PSD is bimodal for TSG, the descriptors of d_{10}, d_{50}, d_{90} will not accurately reflect the changing distribution as they would for a mono-modal distribution but are beneficial nonetheless for denoting trends. For reference, the MRTs determined at the two degrees of fill for this trial were 25 ±1 s (12 % DF - low) and 12 ±1 s (30 % DF - high). The faster process occurring with the higher degree of fill was attributed to the higher space velocity of the powder bed, which is a function of mass flow rate and inversely proportional to screw speed.

The analysis began with direct comparison of the particle size distributions. At 12 % DF, the weight fractions of particles in the size range of 400–1900 μm increased between 30 s to 2 min after startup. By sieving, granules below 400 μm (mainly 102 and 215 μm) decreased in weight fraction after the first measurement at 30 s and then remained unchanged after 1 min (within the limits of uncertainty). After 2 min, which corresponded to five times (5×) MRT at this operating condition, the weight fractions of all particle sizes remained consistent within the limits of uncertainty for sieve classification. By the AE PAT, a decrease in

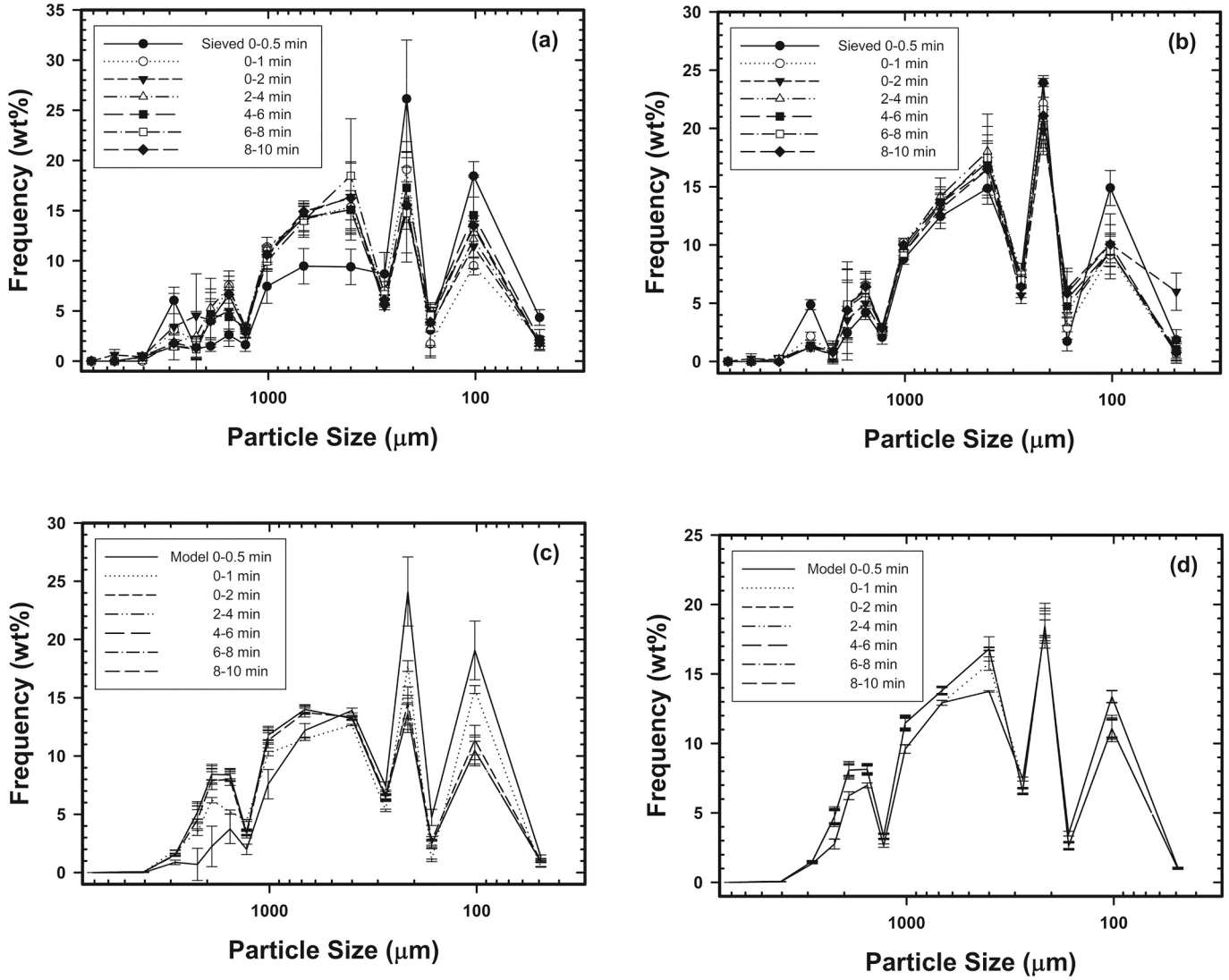

Fig. 4. Particle size distribution by sieving at 27 % L/S ratio with a degree of fill of (a) 12 %, or (b) 30 % with respect to time. Subplots (c) and (d) show the PSD at 27 % L/S ratio from the AE PAT. Error bars for the offline sieved data and PSD estimates represent the standard deviation (n = 3).

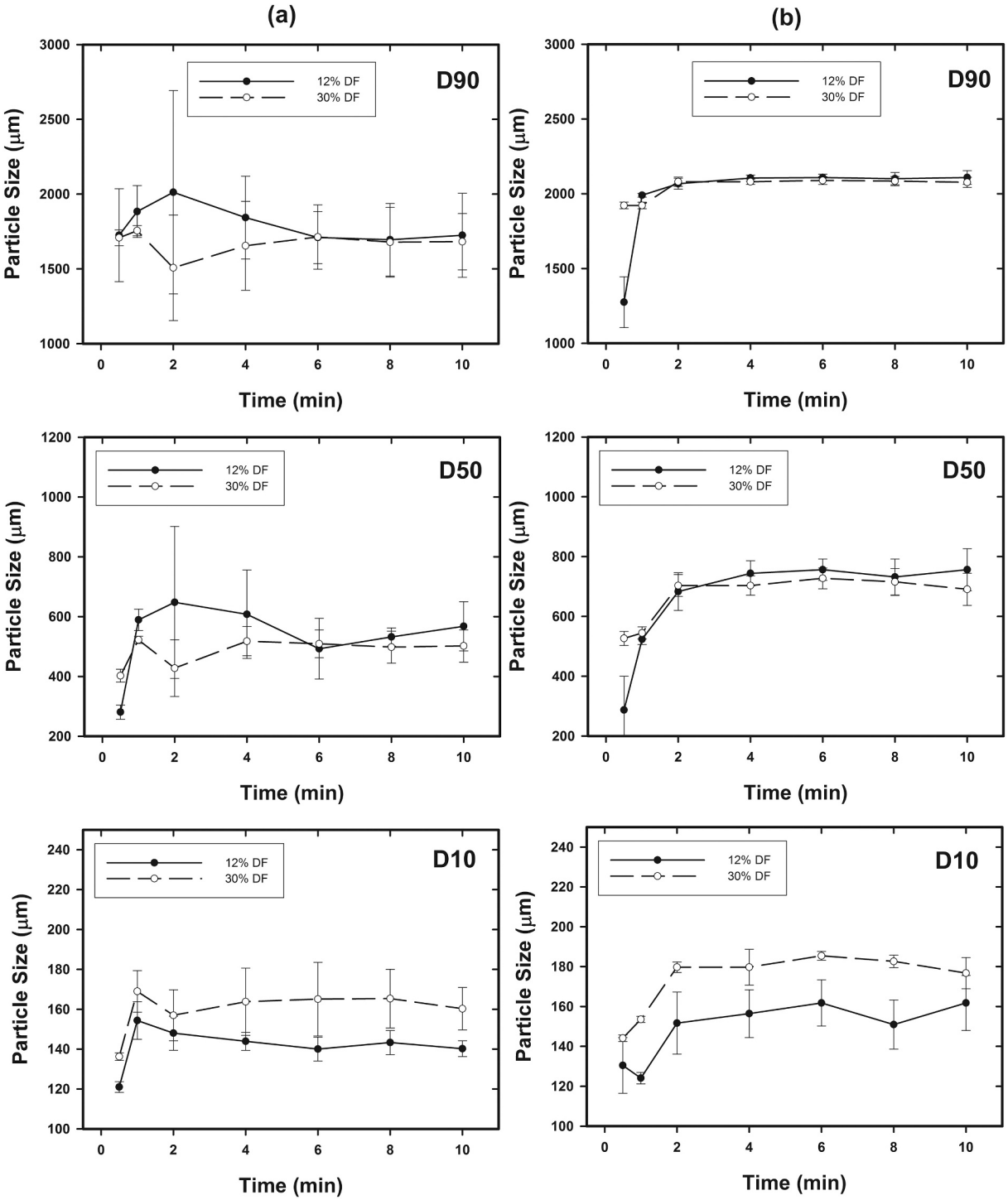

Fig. 5. Plots of the change in d_{90}, d_{50}, and d_{10} with respect to time produced through (a) sieving and (b) AE PAT estimation for 27 % L/S ratio. Error bars represent the standard deviation (n = 3) for both sieved and PAT data.

the fine particles at 102 and 215 μm was noted past 1 min that ceased to change any further after 2 min whereas all size fractions larger than 400 μm show an increase over the same interval. At 30 % DF (high DF), sieved particle sizes showed little variation in their weight fractions from 30 s onwards, with the exception being the 102 μm and 2855 μm sizes that took up to 1 min before they ceased to change further. At this higher DF, the onset of steady state corresponded to 5xMRT, just like at 12 % DF. Using AE PAT, the estimates of weight fractions below 275 μm and above 1015 μm were the same for all time intervals tested with the exception of 9.5–10 min. For the particles sizes corresponding to 400 and 675 μm, the weight fractions increased slightly after 0–0.5 min and then remained constant for all time intervals used, with the exception of 9.5–10 min where another slight increase was observed for all particle sizes above 275 μm. However, the increase was within the uncertainty of the sieved measurements shown in Fig. 4(b). The estimates by PAT corroborated the sieving results that steady state was 5xMRT at the high DF as well.

The three descriptors, d_{10}, d_{50}, d_{90} in Fig. 5 generally represent three distinct regions of the PSD, loosely characterized as fines, desired granules (for tabletting), and coarse particles, respectively from the

granulator. Sieving results for the first 10 min of operation are given in Figs. 5(column 'a') where it is seen that larger versus smaller particle sizes evolved differently while the TSG process was starting up. At low DF, d_{90} and d_{50} increased until 2 min, before slightly decreasing and then no longer changing, whereas the d_{10} increased for 1 min then decreased before becoming constant. This makes sense since it implies fines progressed through the machine at first with little alteration at this degree of fill, while granules took some time to grow but ultimately consumed the fines as would be expected. At high DF, a more consistent trend in the sieved results was observed across all descriptors where the particle size increased until 1 min then decreased before stabilizing. Applying the same mechanistic interpretation as above, this observation implies granule growth did not lag behind at the higher degree of fill, likely indicating less heterogeneity in the wetted state of powders at the site of injection. In comparison, the descriptors determined from the PAT results are given in Figs. 5(column 'b') with smaller error bars. At both DF, d_{90} and d_{50} showed a steep rise in particle size over the first minute and then more gradual granule growth up to 2 min, while d_{10} showed only a gradual increase in size over the 2 min span. The descriptors were constant after 2 min for both DF from the PAT results.

The singular descriptors, by both techniques, did not match the direct observations made of the PSD, with regards to onset of steady state. While the PAT descriptors showed smaller error bars and hence made it clearer as to the trend being seen compared to sieving, the onset of steady state would be much longer in both cases. Due to the bimodal nature of the characteristic PSD from a TSG, these descriptors were amplifying insignificant variances in particle sizes distributed between the two peaks. For this study, the preference was to rely on the findings from direct observation of the PSD and hence, it was concluded that 5xMRT was the most appropriate rule-of-thumb for anticipating the onset of steady state (based on particle size).

The finding of a near-identical onset of steady state with respect to MRT, by the two techniques, for the two DF conditions is ideal by being consistent with transport phenomena principles but was still a novel outcome since there is prior art showing that the granulation mechanism will differ on either side of a transition boundary, found to be ~20 % DF for our process by Shi [16]; the transition boundary corresponds to where a difference has been noted in how screw speed affects particle size in previous process mapping made by Tu et al. [15] and Seem et al. [14]. At 12 % DF, particles are being dragged whereas at 30 % DF, one sees tumbling and avalanching particulate motions. Since we are aware of another transition boundary at a much higher DF(~60 %) where the powder bed becomes much more compressed and begins to move in a plug-like manner [8], one should not assume this rule-of-thumb of 5xMRT for PSD to reach steady conditions necessarily applies to all potential degrees of fill.

Moisture content and fracture strength measured for collected granules from trials at 27 % L/S were examined as functions of time in Fig. 6 to showcase other granule properties relevant for end use. The large error bars seen in Fig. 6(b) are a result of the method of measurement, which involved sampling from a wide particle size range, so a large degree of variability was expected; the large error bars complicate definitively establishing the onset of steady conditions just as they did with the sieved particle size data in Fig. 5 (column 'a'). However, both properties are associated with the collision mechanics of our granules and so their trends helped to understand whether the determined onset of steady state applied to all particle properties. In Fig. 6(a) and (b), at both DF, each analyzed property was found to increase, peak in value and then slightly decrease before becoming mostly constant within their measurement variance. Moisture content became steady after 2 min whereas it was not possible to assess steady results for fracture strength. At 30 % DF, both average moisture content and fracture strength seemed to reach a slightly higher peak value when compared to 12 % DF, which would be reasonably expected by the increased compaction occurring to produce denser granules and are partition liquids from the interstitial regions to the more accessible surfaces of these granules [35,36]. Others have also noted an increase in moisture content at higher DF when studying in-barrel drying of granules within the TSG [37]. The error bars are quite large but with the same trends seen with particle size, we believe it is still reasonable to quote the onset of steady state corresponds to 5xMRT at 12 and 30 % DF.

In summary, the decision to use five times MRT as the onset of steady state was made by accounting for changes in the PSD and its descriptors, as well as granule strength and moisture content observed over the transient period. The size distribution and its descriptors did not change within the limits of uncertainty by 5xMRT at either low or high DF. Fracture strength and moisture content did show greater uncertainties but with similar trends to the PSD descriptors so it was concluded that 5xMRT was appropriate, recognizing that latter collected data never contradicted this definition.

4.3. *Investigation of the transient period of continuous wet granulation by PAT*

The studies in Section 4.2 concluded that steady state of the continuous wet granulation process was best approximated at 60–120 s from startup for the tested formulation, depending on the degree of fill. The analysis of particle classification by sieving in Sec. 4.1 found that at

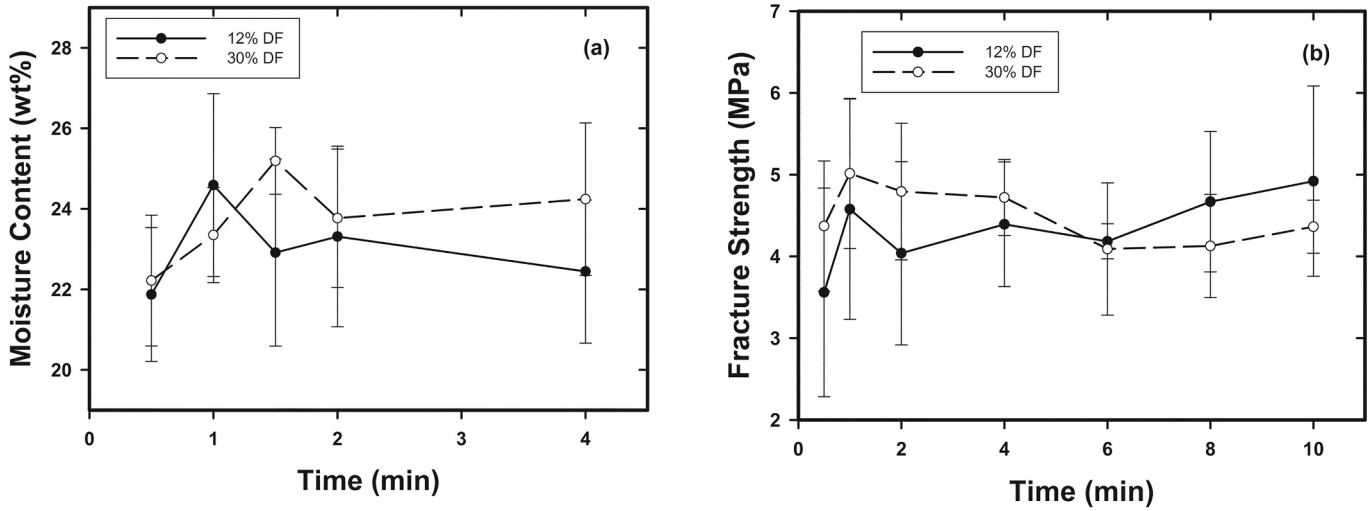

Fig. 6. (a) Moisture content and (b) fracture strength of granules at 27 % L/S ratio as a function of time. Error bars represent the standard deviation (n = 3).

least 20 g of material was required to reliably produce a PSD by the method, which translates to a minimum of 16 or 24 s of material sampling at the high and low DF examined in this study, respectively. Comparably, a reliably produced PSD by AE PAT was found between 5 and 10 s of signal sampling. This meant offline sieving would provide a lower resolution of information, concerning evolving PSD during the transient period compared to the inline PAT. Despite this higher rate of process monitoring possible by PAT, neither PAT nor sieving can begin sample collection until material begins to leave the machine. For this study, time equivalent to 1xMRT was allowed to pass before analysis of the acoustic signal was considered, which meant the first PSD was estimated 5 s after MRT in the results of this section (namely 30 s or 20 s for 12 % or 30 % DF, respectively). It is for this reason that many particle sizes in Fig. 7, while changing over the remaining 4xMRT, appear to near instantly grow in weight fraction at time corresponding to 1xMRT; that jump in weight fraction will be ignored (data not shown) in the analysis since it is an artefact of the monitoring method. Fig. 7 shows the change in two representative particle sizes over time for fractions identified as fines (102 μm, 215 μm), desired granulates (675 μm, 1015 μm), and coarse granules (1900 μm, 2230 μm). The plot shows the evolving PSD for the well studied 27 % L/S ratio as well as the PSDs for 18 % L/S and 39 % L/S using signal data collected from their trials to train the AI

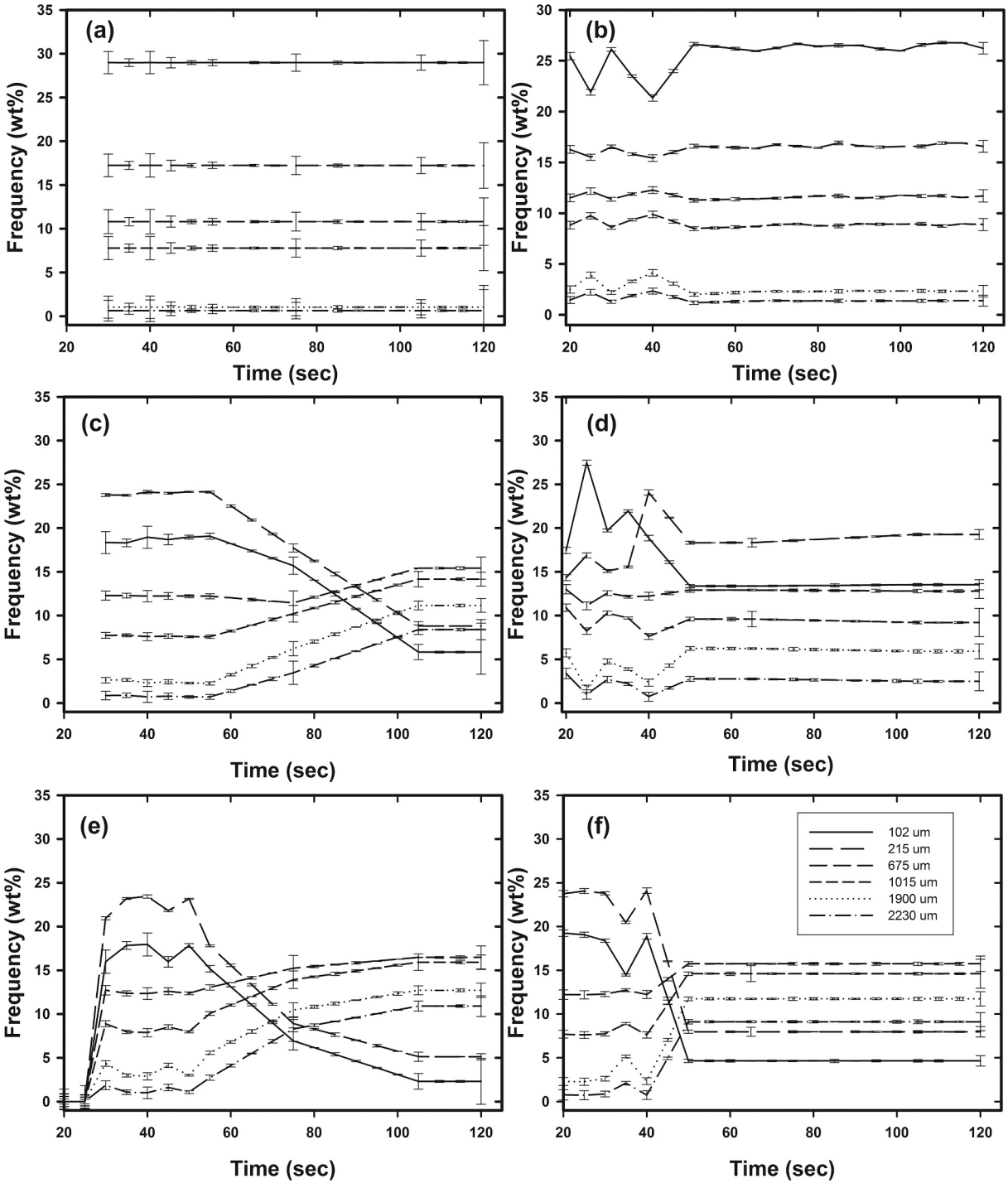

Fig. 7. Change in particle size over time using the AE PAT from 1xMRT up to 120 s at 12 % DF at (a) 18, (c) 27, (e) 39 % L/S ratio. Subplots (b), (d), and (f) at 30 % DF correspond to the same L/S ratios (18, 27, and 39 %, respectively).

model.

Using 18 % L/S ratio, at either degree of fill, one observed little-to-no variation in the PSD as a function of time. At the high DF, a little more variation was observed over 30–45 s, with the weight fraction of 102 μm (nominally) sized powder decreasing and then increasing until it remained essentially constant; whenever this particle size decreased, a small increase in weight fraction was observed for the 675 μm, 1015 μm, 1900 μm, and 2230 μm sizes. The insignificant change at 18 % L/S at both degrees was likely because the liquid content was too low for significant granule growth; at least ~60 % of the particle sizes remained ungranulated (<400 μm) even at steady state.

At the two higher L/S ratios, there was much more variation in the different granule sizes over time making up the PSD and more distinction between the two degrees of fill. At 12 % DF, the weight fraction of fines (102 μm and 215 μm) dominated the PSD over the period of 30–60 s (~1.0–2.0xMRT) for all L/S ratios. From 60 to 90 s (~2.0–4.2xMRT) the fines decreased in their weight fraction, down to about 7 wt% with 27 % L/S ratio or 4 wt% with 39 % L/S ratio, and then remained constant at its steady state value from 105 to 120 s (~4.2-5xMRT). For the desired granule sizes (675 μm and 1015 μm) and coarse sizes (1900 μm and 2230 μm) the weight fractions remained steady from ~1.0–2.0xMRT and then increased to its steady state values at ~16 and ~ 12 wt%, respectively, from 2 to 4.2xMRT at both L/S ratios. At 30 % DF, the fines with 27 % L/S ratio showed some variance between 20 and 50 s (~1.0-4xMRT) as but leveled off at ~15 wt%. The other size groups (675 μm, 1015 μm, 1900 μm, and 2230 μm) showed small increases over this same period of time, with the coarse granule size corresponding to 1900 μm showing the greatest increase in weight fraction up to 6 wt%. At 39 % L/S ratio, the fine fractions underwent a drastic decrease from 40 to 50s from ~20 wt % to 6 wt%. All other weight fractions shown in Fig. 7 underwent a sharp growth at this binder concentration after 40 s and then remained constant after 50 s, with the largest particle fractions being at 675 μm and 1015 μm (both around 14–15 wt%) followed by 2230 μm and 1900 μm (9–11 wt%).

4.4. Granulation mechanism

The transient behaviour discussed is based on results in Section 4.3 and observations after material began to exit the extruder (i.e. ~1xMRT). Fines being the fed solids into the machine, were dominant (~40 wt%) in the earliest stages of startup (1-2xMRT) for both DF, with no significant granulation evident; with little binder built up on the barrel wall in the kneading zone to cause viscous drag, most of the powder will pass through the influential zone without the local decrease in velocity necessary to cause bed compaction. Beyond this period, differences in granule development were noted in the exiting PSD based on degree of fill, except at 18 % L/S ratio which was too dry to consider in this analysis of the granulation mechanism.

At 12 % DF, after a period corresponding to an additional MRT had passed, the binder wetted particles showed evidence of coalescing into larger granules according to the AE PAT. With so little available volume occupied at this condition, the powder is only being dragged forward by the flight, free to roll, jostle about, and stick with other particles in the conveying zone. It was actually difficult to see the influence of the kneading zone at this low DF with only gradual granule growth seen from ~2–4.2xMRT since compaction should bring about the rapid development of large, even coarse, particles. The poor compaction may be caused by insufficient liquid being squeezed out to coat the barrel in the kneading zone (for viscous drag) and/or insufficient volume to cause pressurization in that zone to create strong enough granules to not breakup in the subsequent conveying zone. At both moderate and high binder concentrations (27 and 39 % L/S ratio in this case) the AE PAT showed granule growth at this DF was a gradual process, since granules up to 1015 μm and 1900 μm were formed. Gradual growth seemed to be characteristic of this low DF while the binder content added determined whether the PSD favored larger sizes.

At 30 % DF, increasing the mass flowrate at a fixed screw speed increases the volume occupied by the powder in the screws. Interestingly, the collected particles starting after 1xMRT showed less change in weight fraction over time than seen at the lower DF, especially for a binder concentration below 39 % L/S ratio. In the conveying zone, the powder will continue to be dragged by the flights of the screws but collisions arising from such jostling would be reduced (though still expectedly possible due to shear dilatancy) while some portion of the powder bed may now be thrown over the screw root, moving solids with greater frequency from one screw to the other. The increased bed density at this higher DF is thought to promote growth by allowing more compressive forces to build across the kneading zone and in the upstream conveying elements, causing consolidation of the wetted particles exhibiting higher inter-particle forces [38,39]. At the moderate binder concentration (27 % L/S), particle growth was only seen at 275 μm from ~1-4xMRT whereas all other sizes seem to be produced to their steady state weight fraction prior to 1xMRT. At the highest binder content of this study (39 % L/S ratio), there was a larger degree of change for the fines, desired granulates, and coarse size fraction but after some delay. At ~3-4xMRT, a very sharp growth in granules was seen while fines were correspondingly reduced, unlike the gradual nature seen at 12 % DF. This wetting condition was the first definitive instance where the kneading zone was felt to be significantly contributing to the size and strength of granules produced; the zone does not produce a compacted mass until sufficient liquid slows particle movement through the zone and sufficient powder tried to pass through the zone. The kneading zone has been reported in other studies to be where intense compaction occurs over a very short distance, once densification begins [39]. The rapid rise in larger granules at ~3-4xMRT can not be explained by conveying, which would have been occurring since startup. A similar effect during steady operations was seen by Vercruysse et al. [9] where they varied the number of kneading elements in the screw design at multiple fill levels and found that increasing the number of kneading elements increased the time to grow coarse granules (above 1400 μm).

Finally, in consideration of the transition boundary (~20 % DF), where the growth mechanism changes based on its dependency on screw speed [14–16], we note the major difference in PSD development on either side is the rate at which larger particles grow. Despite the blackbox nature of the process, we believe the transient period is showing a stronger influence of the kneading zone on granule growth above 20 % DF, where screw speed has little effect on particle size; below 20 % DF, we believe the conveying zone has a stronger influence on granule growth, consistent with the slower growth along the length of the screws and for which the influence of screw speed is most obvious, undampened by the downstream kneading zone.

5. Conclusion

A study was conducted to observe the transient evolution of the particle size distribution produced by twin screw wet granulation from process startup until steady state, using offline mechanical sieving versus a newly-developed inline acoustic-based PAT. Observing the PSD over time at low and high degrees of fill by both techniques, it was determined that steady state corresponded to roughly five times the mean residence time of the process. Due to measurement variability, there was less certainty that other granule properties such as moisture content and fracture strength, had become steady in the same period of time. Through detailed evaluations of both particle size characterization techniques, the PAT method was ultimately chosen to study the transient period of process startup to learn more about the wet granulation mechanism in a TSG because it could estimate PSD over a shorter period of sampling. At a low degree of fill it was found that the conveying zone seemed to have a stronger impact on granule size on account of the gradual growth witnessed at moderate to high binder contents. Comparatively, at a high degree of fill, it was found that the kneading

zone became a stronger contributor to granule development due to the rapid increase in the weight fraction of large granules after a hold up period for the fines over 1-2xMRT. From this work it is believed that liquid distribution, formulation behaviour, and screw design can influence growth behaviour, so future studies will focus on exploring different wetting methods (2nd injection port, foam granulation), formulation elasticity, as well as changes in screw design and temperature along with their impact on the granulation mechanism.

CRediT authorship contribution statement

H.A. Abdulhussain: Writing – original draft, Software, Methodology, Investigation, Formal analysis, Data curation. **M.R. Thompson:** Writing – review & editing, Supervision, Project administration, Methodology, Funding acquisition, Conceptualization.

Declaration of competing interest

The authors declare the following financial interests/personal relationships which may be considered as potential competing interests:

Michael Thompson reports financial support was provided by Natural Sciences and Engineering Research Council (NSERC). Michael Thompson reports equipment, drugs, or supplies was provided by BASF Corp. Michael Thompson reports equipment, drugs, or supplies was provided by International Flavors & Fragrances Inc. If there are other authors, they declare that they have no known competing financial interests or personal relationships that could have appeared to influence the work reported in this paper.

Data availability

The data that has been used is confidential.

Acknowledgements

The authors would like to thank Kevin O'Donnell and International Flavors and Fragrances Inc. (formerly Dow Chemical) for donating the lactose monohydrate, and Shaukat Ali and BASF for donating the Kollidon SR used in this study. We would like to thank the Natural Sciences and Engineering Research Council of Canada (NSERC) for its funding of this work. Additionally, our thanks goes to Dr. Prashant Mhaskar for consulting extensively on how the AI model handles its large datasets.

References

[1] V. Pauli, P. Kleinebudde, M. Krumme, From powder to tablets: investigation of residence time distributions in a continuous manufacturing process train as basis for continuous process verification, Eur. J. Pharm. Biopharm. 153 (2020) 200–210.
[2] L. Kotamarthy, C. Sampat, R. Ramachandran, Development of a granule growth regime map for twin screw wet granulation process via data imputation techniques, Pharmaceutics 14 (2022) 2211.
[3] K.T. Lee, A. Ingram, N.A. Rowson, Twin screw wet granulation: the study of a continuous twin screw granulator using positron emission particle tracking (PEPT) technique, Eur. J. Pharm. Biopharm. 81 (2012) 666–673.
[4] R.M. Dhenge, J.J. Cartwright, M.J. Hounslow, A.D. Salman, Twin screw granulation: steps in granule growth, Int. J. Pharm. 438 (2012) 20–32.
[5] M. Verstraeten, D. Van Hauwermeiren, K. Lee, N. Turnbull, D. Wilsdon, M. Ende, P. Doshi, C. Vervaet, D. Brouckaert, S.T.F.C. Mortier, I. Nopens, T.D. Beer, In-depth experimental analysis of pharmaceutical twin-screw wet granulation in view of detailed process understanding, Int. J. Pharm. 529 (2017) 678–693.
[6] R.M. Dhenge, K. Washino, J.J. Cartwright, M.J. Hounslow, A.D. Salman, Twin screw granulation using conveying screws: effects of viscosity of granulation liquids and flow of powders, Powder Technol. 238 (2013) 77–90.
[7] L. Vandevivere, E. Van Wijmeersch, O. Häusler, T. De Beer, C. Vervaet, V. Vanhoorne, The effect of screw configuration and formulation variables on liquid requirements and granule quality in a continuous twin screw wet granulation process, J. Drug Deliv. Sci. Technol. 68 (2022) 103042.
[8] M.R. Thompson, J. Sun, Wet granulation in a twin-screw extruder: implications of screw design, J. Pharm. Sci. 99 (2010) 2090–2103.
[9] J. Vercruysse, D. Córdoba Díaz, E. Peeters, M. Fonteyne, U. Delaet, I. Van Assche, T. De Beer, J.P. Remon, C. Vervaet, Continuous twin screw granulation: influence of process variables on granule and tablet quality, Eur. J. Pharm. Biopharm. 82 (2012) 205–211.
[10] M.R. Thompson, Twin screw granulation – review of current progress, Drug Dev. Ind. Pharm. 41 (2015) 1223–1231.
[11] A. Kumar, J. Dhondt, J. Vercruysse, F. De Leersnyder, V. Vanhoorne, C. Vervaet, J. P. Remon, K.V. Gernaey, T. De Beer, I. Nopens, Development of a process map: a step towards a regime map for steady-state high shear wet twin screw granulation, Powder Technol. 300 (2016) 73–82.
[12] A. Kumar, J. Vercruysse, M. Toiviainen, P.-E. Panouillot, M. Juuti, V. Vanhoorne, C. Vervaet, J.P. Remon, K.V. Gernaey, T. De Beer, I. Nopens, Mixing and transport during pharmaceutical twin-screw wet granulation: experimental analysis via chemical imaging, Eur. J. Pharm. Biopharm. 87 (2014) 279–289.
[13] D. Djuric, P. Kleinebudde, Continuous granulation with a twin-screw extruder: impact of material throughput, Pharm. Dev. Technol. 15 (2010) 518–525.
[14] T.C. Seem, N.A. Rowson, A. Ingram, Z. Huang, S. Yu, M. de Matas, I. Gabbott, G. K. Reynolds, Twin screw granulation — a literature review, Powder Technol. 276 (2015) 89–102.
[15] W.-D. Tu, A. Ingram, J. Seville, Regime map development for continuous twin screw granulation, Chem. Eng. Sci. 87 (2013) 315–326.
[16] Z. Shi, Understanding Scalability in a Twin Screw Wet Granulation, Chemical Engineering, McMaster University, 2022. http://hdl.handle.net/11375/27950.
[17] J. Vercruysse, U. Delaet, I. Van Assche, P. Cappuyns, F. Arata, G. Caporicci, T. De Beer, J.P. Remon, C. Vervaet, Stability and repeatability of a continuous twin screw granulation and drying system, Eur. J. Pharm. Biopharm. 85 (2013) 1031–1038.
[18] A. Ryckaert, F. Stauffer, A. Funke, D. Djuric, V. Vanhoorne, C. Vervaet, T. De Beer, Evaluation of torque as an in-process control for granule size during twin-screw wet granulation, Int. J. Pharm. 602 (2021) 120642.
[19] H.A. Abdulhussain, M.R. Thompson, Considering inelasticity in the real-time monitoring of particle size for twin-screw granulation via acoustic emissions, Int. J. Pharm. 639 (2023) 122949.
[20] W.-J. Wang, D. Yan, S. Zhu, A.E. Hamielec, Kinetics of long chain branching in continuous solution polymerization of ethylene using constrained geometry metallocene, Macromolecules 31 (1998) 8677–8683.
[21] M. Zhang, T.W. Karjala, B.W.S. Kolthammer, Delayed dynamics of polymer properties in continuous stirred tank polymerization reactors, Ind. Eng. Chem. Res. 46 (2007) 5922–5935.
[22] A.J. Alvarez, A.S. Myerson, Continuous plug flow crystallization of pharmaceutical compounds, Cryst. Growth Des. 10 (2010) 2219–2228.
[23] C.J. Brown, J.A. Adelakun, X.-W. Ni, Characterization and modelling of antisolvent crystallization of salicylic acid in a continuous oscillatory baffled crystallizer, Chem. Eng. Process. Process Intensif. 97 (2015) 180–186.
[24] BASF, Kollidon® SR | Coprocessed Excipients | BASF Pharma, BASF, 2023. https://pharma.basf.com/products/kollidon-sr.
[25] S. Mozumder, Scale-Up of Pharmaceutical Twin-Screw Wet Granulation Based on the Process Simulation Using Genetic Programming, Chemical Engineering, McMaster University, 2023. http://hdl.handle.net/11375/28417.
[26] S.V. Lute, R.M. Dhenge, A.D. Salman, Twin screw granulation: an investigation of the effect of barrel fill level, Pharmaceutics 10 (2018) 67.
[27] M.J. Adams, M.A. Mullier, J.P.K. Seville, Agglomerate strength measurement using a uniaxial confined compression test, Powder Technol. 78 (1994) 5–13.
[28] H.A. Abdulhussain, M.R. Thompson, Predicting the particle size distribution in twin screw granulation through acoustic emissions, Powder Technol. 394 (2021) 757–766.
[29] P. Acoustics, F30a - 150-750 kHz High-Sensitivity Flat Frequency Response AE Sensor, by Physical Acoustics. https://www.physicalacoustics.com/by-product/sensors/F30a-150-750-kHz-High-Sensitivity-Flat-Frequency-Response-AE-Sensor, 2024.
[30] A.J. Hickey, T.M. Crowder, M.D. Louey, N. Orr, A Guide to Pharmaceutical Particulate Science, 1st ed, CRC Press, 2003, https://doi.org/10.1201/9780203009673.
[31] H.G. Merkus, Particle Size Measurements: Fundamentals, Practice, Quality, 1st ed, Springer Science & Business Media, 2009, https://doi.org/10.1007/978-1-4020-9016-5.
[32] E. Franceschinis, V. Bressan, E. Fontanel, N. Realdon, S. Volpato, A.C. Santomaso, Effect of the drying type on the properties of granules and tablets produced by high shear wet granulation, Powder Technol. 434 (2024) 119316.
[33] S. Oka, H. Emady, O. Kašpar, V. Tokárová, F. Muzzio, F. Štěpánek, R. Ramachandran, The effects of improper mixing and preferential wetting of active and excipient ingredients on content uniformity in high shear wet granulation, Powder Technol. 278 (2015) 266–277.
[34] A. Ryckaert, M. Ghijs, C. Portier, D. Djuric, A. Funke, C. Vervaet, T. De Beer, The influence of equipment design and process parameters on granule breakage in a semi-continuous fluid bed dryer after continuous twin-screw wet granulation, Pharmaceutics 13 (2021) 293.
[35] T. Monteyne, J. Vancoillie, J.-P. Remon, C. Vervaet, T. De Beer, Continuous melt granulation: influence of process and formulation parameters upon granule and tablet properties, Eur. J. Pharm. Biopharm. 107 (2016) 249–262.
[36] A. Pradhan, M. Costello, F. Yang, V. Bi, T. Durig, F. Zhang, Using twin-screw melt granulation to co-process mannitol and hydroxypropylcellulose, J. Drug Deliv. Sci. Technol. 77 (2022) 103880.

[37] A. Haser, N. Kittikunakorn, E. Dippold, J.C. DiNunzio, W. Blincoe, Continuous twin-screw wet granulation process with in-barrel drying and NIR setup for real-time moisture monitoring, Int. J. Pharm. 630 (2023) 122377.

[38] D. Djuric, B. Van Melkebeke, P. Kleinebudde, J.P. Remon, C. Vervaet, Comparison of two twin-screw extruders for continuous granulation, Eur. J. Pharm. Biopharm. 71 (2009) 155–160.

[39] H. Li, M.R. Thompson, K.P. O'Donnell, Understanding wet granulation in the kneading block of twin screw extruders, Chem. Eng. Sci. 113 (2014) 11–21.